Stress softening behaviour of HDNR bearings: modelling and influence on the seismic response of isolated structures

Stress-softening behaviour of HDNR bearings: modelling and influence on the seismic response of isolated structures

Enrico TUBALDI [1], Laura RAGNI [2], Andrea DALL'ASTA[3], Hamid AHMADI[4] , Alan MUHR[4]

[1] Department of Civil and Environmental Engineering, Imperial College London, London, UK; email: etubaldi@ic.ac.uk

[2] Department of Construction, Civil Engineering and Architecture, Polytechnic University of Marche, Via Brecce Bianche Ancona (AN), Italy; E-mail: laura.ragni@univpm.it.

[3] School of Architecture and Design, University of Camerino, Viale della Rimembranza, 63100 Ascoli Piceno (AP), Italy; E-mail: andrea.dallasta@unicam.it

[4] Tun Abdul Razak Research Centre (TARRC), Brickendonbury, Brickendon Lane, Hertford SG13 8NL, UK hahmadi@tarrc.co.uk; amuhr@tarrc.co.uk

SUMMARY

High damping natural rubber (HDNR) bearings are extensively employed for seismic isolation of structures because of their low horizontal stiffness and high damping capacity. Filler is used in HDNR formulations to increase the dissipative capacity, and it induces also a stress-softening behaviour, known as the Mullins effect. In this paper, a wide experimental campaign is carried out on a large number of virgin HDNR samples to better investigate some aspects of the stress-softening behaviour, such as the direction-dependence and recovery properties, and to characterize the stable and softening response under different strain histories. Test results are also used to define a model for simulating the response of HDNR bearings in shear that advances the state of the art in the description of the stress-softening, which can be significant during the earthquake time-history. The proposed model is used to analyse the seismic response of a simplified isolated structure modelled as a S-DOF system under ground motions with different characteristics and by considering two different conditions for the bearings: one assuming the virgin (or fully recovered) rubber properties and the other assuming the stable (or fully scragged) rubber properties. The results show that, in the case of far field records, the differences between the responses are limited although not negligible, whereas for near fault records, modelling the bearings as being in their virgin state significantly reduces the effect of this kind of motion on isolated structures.

KEYWORDS: high damping natural rubber, seismic isolation, Mullins effect, stress-softening

INTRODUCTION

In the last few decades, laminated high damping natural rubber (HDNR) bearings have been extensively employed for seismic isolation of buildings and bridges because of their low horizontal stiffness and high damping capacity, which enable the isolated vibration period to be shifted away from the range where the earthquake input has the highest energy content and most of the relative displacements to be accommodated benignly, and reduced through dissipation of energy taking place in the bearings rather than in the structure.

The seismic response of a system isolated with HDNR bearings is mainly controlled by the HDNR material behaviour in simple shear, which is characterized by different specific features such as dependency on the strain-amplitude (Payne or Fletcher & Gent effect), stiffening at large strains due to crystallization, stress-softening due to repeated cycles, a generally mild strain rate sensitivity, as well as dependency on environmental factors such as long term ageing and ambient temperature. In particular stress-softening, on which this paper is focused, may be considered as a macroscopic consequence of breakdown of filler-filler structure and rubber-filler interaction which takes place within the "virgin" rubber during the deformation-path. This effect, whose extent depends on the maximum strain amplitude the material has been subjected to during loading cycles and does not much affect the loading curve for strains higher than the maximum strain experienced [1], is often

referred to in the literature as the "Mullins effect" [2] whereas the process of generating such softening effect is often referred to as "scragging" [3], being a procedure sometimes applied to metal springs or rubber mounts after production and before service. The largest softening effect occurs in the first cycle, and models for the "Mullins effect" usually focus on this (e.g. [2]); softening on subsequent cycles to the same strain has been referred to as "cyclic stress relaxation" [4] or "continuous damage" [5]. However, Clark et al. [6], with reference to cyclic loading paths at a given strain amplitude. use the term "scragging" to denote the softening characterizing the first cycle, and "Mullins effect" for the softening over the other cycles. As such classification is not consistent in the rubber science literature, thus all the softening effects are termed here as the "Mullins effect", and will also be modelled in a unified way. It is sometimes thought that stress-softening effects can be eliminated by subjecting HDNR-based devices to several cycles at a large shear amplitude, i.e. scragging, as part of a manufacturer's quality control practices. However, experimental evidence has shown that the rubber can at least partially recover its initial (or "virgin") stress-strain properties over time [3,7-9]. The recovery behaviour is usually rapid at the beginning, and continues at slower rates. It is known that the rate of the recovery depends on several factors, such as the elastomeric compound, the manufacturing process and the temperature, however comprehensive recovery models have not been developed yet. Since an earthquake may occur after a long period of rest of the isolation system, when a seismic event occurs the properties of the bearings could have fully recovered to the virgin state, thus the evaluation of the seismic reliability of HNDR isolated structures would require dynamic analyses accounting for softening from the virgin state during the strong motion, as also experimentally observed [10,11].

Many different three-dimensional large strain constitutive models of filled rubber have been made available [12-15]. In some cases the Mullins effect has been included by coupling continuum damage theory with elasticity theory [12], viscoelasticity theory [13], or pseudo-elasticity theory [15]. These material models permit a detailed description of the behaviour of laminated HDNR bearings up to collapse via finite element analysis. However, this approach is too complex for engineering applications. For this reason, several device phenomenological models have been proposed in the past to describe the global behaviour of HDNR bearings. At this regard, it is found, to a good approximation, that for typical design of laminated rubber bearings (e.g., primary shape factor $S_1>20$ and secondary shape factor $S_2>3$, [16,17]) and under typical design axial loads, bending moments, and shear deflections (far from collapse condition as imposed by Standards), the shear load-deflection behaviour of a laminated HDNR bearing is the same as that of a block, constrained to be in simple shear, of the same total thickness, cross-sectional area and material properties as the rubber in the bearing. In fact, under these conditions the effects of axial load and bending moment on the shear-load behaviour of such a single rubber layer in the bearing are negligible and the extra compliance resulting from P-Δ effects estimated from the appropriate beam-column theory can be assumed to be small. Consequently, several device phenomenological models have been proposed in the past to describe the behaviour of the HDNR bearings in simple uniaxial shear [18-22] and biaxial shear [23-25]. Obviously, in the near collapse conditions more complex stress states of the isolation device will arise. However, device phenomenological models can still be used to globally describe the multiaxial behaviour of bearings [26-28], by accounting for specific relevant phenomena, such as the cavitation/buckling occurring under tensile/compression strains as well as coupling effects between the horizontal and vertical behaviour.

However, few models among those mentioned take into account the stress-softening process occurring during cyclic loadings. In particular, in the model proposed by Kikuchi and Aiken [19] and then adopted in Kikuchi et al. [27] this process is accounted for in a simplified way by introducing an additional elastic force which vanishes when the current shear strain is within the minimum and maximum strains already experienced in the past. Differently, in Hwang et al. [20] the stress-softening is modelled by using load-history dependent parameters whereas in Grant et al. [24-25] and Dall'Asta and Ragni [22] it is accounted for through damage parameters evolving as the strain history progresses. However, recent experimental investigations have shown that the

stress-softening is direction-dependent, in the sense that cyclic loadings in one direction (i.e., for positive or negative strains) only marginally affect the stresses in uniaxial cyclic loadings in the other direction [29-30]. This direction-dependent behaviour, which may influence significantly the response of HDNR bearings under generic strain histories, is the subject of very recent research and it has not been included yet in device models.
This paper describes the experimental campaign carried out on HDNR double-shear specimens, manufactured by TARRC from a highly dissipative rubber compound commonly employed for seismic isolators, to better understand and model the stress-softening which might significantly affect the seismic response of structures isolated on virgin HDNR bearings. The choice of employing small test pieces is motivated by the large number of independent tests that have to be carried out on separate virgin HDNR samples to achieve a satisfactory characterization of the stress softening of HDNR, which would result in a prohibitive cost if full-scale devices were employed. Moreover, as already explained, for typical bearing geometries and loading conditions, the material behaviour in shear can be assumed to represent the horizontal behaviour of virgin HDNR bearings. In the first part of the paper the results of uniaxial tests are illustrated and discussed. Next, a one-dimensional non linear process-dependent constitutive model is described, which advances the model previously developed by some of the authors for HDNR devices [22]. The proposed model provides a better description of the transient behaviour of the rubber (characterizing the transition from the virgin state to the damage stabilization) by accounting also for the direction-dependence of the Mullins effect and thus it can be used to accurately simulate the shear response of HDNR bearings under transient motions.
In the last part of the paper the model is employed to evaluate the influence of stress softening on the seismic response of isolated structures under design conditions. In fact, despite the relevance of this topic especially for strategic isolated structures, few studies have been carried out thus far to evaluate the effects due to the softening in cyclic shear loading on the seismic reliability assessment of isolated systems. Some preliminary investigations have been done by Stewart et al. [10] based on experimental testing and by Dall'Asta and Ragni [31-32] based on numerical simulations. In this paper, further numerical investigations are carried out by considering an isolated structure modelled as a S-DOF system and by performing several dynamic analyses under different seismic inputs, including near-fault (NF) and far-field (FF) records, producing different strain paths. In all the analyses, two different limit conditions have been considered to highlight the influence of the Mullins effect: (*i*) the case of virgin bearings and (*ii*) the case where stress-softening is fully developed to the maximum strain expected during the motion. Although this last case is primarily a limit condition for the rubber, given the partial or total recovery occurring during the interval time between the manufacturer's quality controls and an earthquake or between two earthquakes, it serves as a limit state for the purposes of comparison to highlight the effects of stress-softening on the seismic response of isolated structures and to evaluate the differences between the responses obtained by considering or neglecting the effects of stress-softening during the seismic time-history.

EXPERIMENTAL TESTS

The experimental campaign described in this paper has been carried out on a large number of identical virgin material double shear testpieces (see Figure 1).They were manufactured by TARRC from a highly dissipative rubber compound commonly employed for seismic isolators, that satisfies the prescriptions of the current European code EN15129 [33] for anti-seismic devices about the stability of shear properties under repeated cycling, as well as similar prescriptions of other international seismic codes such as AASHTO 2010 [34] or ASCE/SEI 41-139 [35].
The tests have been tailored to characterize the transient and stable behaviour of the rubber in uniaxial simple shear under different strain amplitudes and strain rates and to study some aspects related to the Mullins effect, such as the direction-dependence and the recovery properties. In the following sections, after a brief description of the double shear test set-up, the main results of the experimental campaign are reported.

Test set-up

The testpiece for double-shear tests consist of two cylindrical rubber discs (Fig.1a) moulded between three metal end pieces. The thickness t of the disc is 6mm and its diameter D is 25mm, since standards for testing rubber ([33],[36]) stipulate for shear tests a value $D/t > 4$ to render imperfections in the boundary conditions insignificant so that the rubber can be taken to be mainly in uniform simple shear. The central metal cylinder is driven by a servohydraulic actuator, while the end pieces are held in a jig attached to a load cell fixed to the machine bed. (Fig. 1b). The testing machine's internal sensors record the load cell force and the imposed displacements during the test. It is noteworthy that the shear deformations reported in the figures include also the deformation of the steel rod and of the strain gauges in the load cell, whose contribution is however negligible.

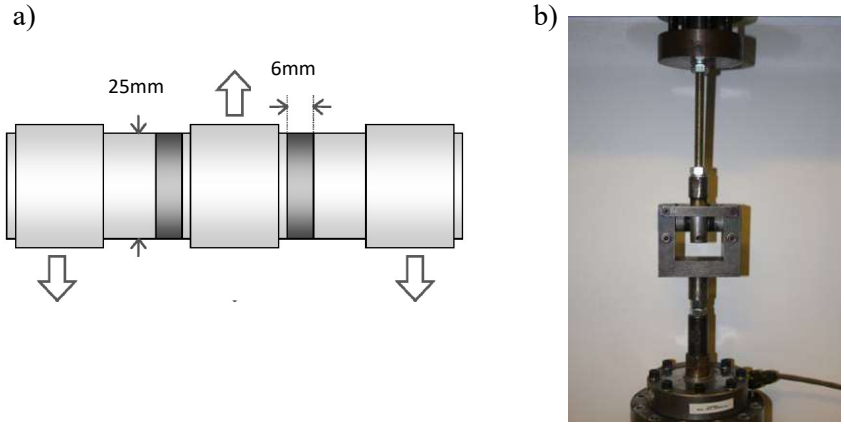

Fig. 1- Test set-up: (a) double shear test piece geometry; (b) test machine

Double shear tests for the rubber behaviour characterization

The current European code EN15129 [33] for anti-seismic devices prescribes that the ratio between the minimum and maximum value of the secant shear modulus G measured in the cycles between the 1st and the 10th shall not be less than 0.6 at the design shear strain. To verify the compliance of this prescription, the first test of the experimental campaign was a sinusoidal test carried out at the maximum strain amplitude γ_{max} = 1.5, which is the assumed design amplitude, and frequency 0.5 Hz. Results are reported in Fig. 2a, in terms of shear stress (τ) versus the shear strain (γ), calculated by dividing the measured force and displacement respectively by the total cross-section area and the thickness of the testpiece. The shear modulus, defined as $G = \tau_{max}/\gamma_{max}$, for $\gamma_{max} = 1.5$ is G_1 = 1.03 MPa at the 1st cycle, G_3 = 0.752 MPa at the 3rd cycle, and G_{10} = 0.653 MPa at the 10th cycle. Although the stress-softening under repeated cycling is significant, the ratio $r=G_{10}/G_1=0.62$ (also defined in Fig.2a), is higher than the minimum threshold value of 0.6 allowed by the European code. Note also that the rubber compound has an equivalent damping ratio at the 10th cycle of 0.16. It is worth noting that the ratios of $r=G_{10}/G_1$ for shear strains measured in the range of 100% to 250% are all above 0.6.

In order to investigate the damage evolution characterizing the transient behaviour of the virgin rubber and its dependence on the maximum strain amplitude experienced, a first series of cyclic tests with triangular waveform was carried out at different deformations (γ_{max}) and at different strain rates ($\dot{\gamma}$) kept constant during each test, with no pauses between continued positive or negative strain ramps. In particular, two tests were firstly performed at $\gamma_{max} = 2.5$, which was the highest deformation considered in any test, and with strain rates equal to $\dot{\gamma} = 1s^{-1}$ and $\dot{\gamma} = 4s^{-1}$. More in detail, 20 cycles at the amplitude $\gamma_{max} = 2.5$ and further 20 cycles at successively smaller amplitudes equal to 2, 1.5, 1, 0.5 and 0.25 were imposed. In Fig. 2b, the stress-strain loops relevant

to the test with $\dot{\gamma} = 1s^{-1}$ are reported. The objective of this type of test was to determine the "primary curve" of the virgin material (i.e. the loading path of the first cycle) and to analyze how the stress softening progresses up to stable cycles at the maximum assumed deformation $\gamma_{max} = 2.5$. The hysteresis cycles change very little after 10-15 cycles of imposed strain, and the temperature increment (calculated from the dynamic results assuming adiabatic heating of the rubber) is negligible and thus does not influence the results significantly for this number of cycles. It can be observed in Fig. 2b that once the stress-softening is stabilized for the cycles at the maximum amplitude of deformation, successive cycles at smaller amplitudes are also stable and they are all "included" in the largest stable cycle since their stiffness is influenced by the extent of stress softening that occurred at the maximum experienced strain ($\gamma_{max} = 2.5$). However, the stiffness of the stable cycles increases for decreasing strain amplitude, a behaviour which is commonly referred to as Payne or Fletcher & Gent effect in the literature.

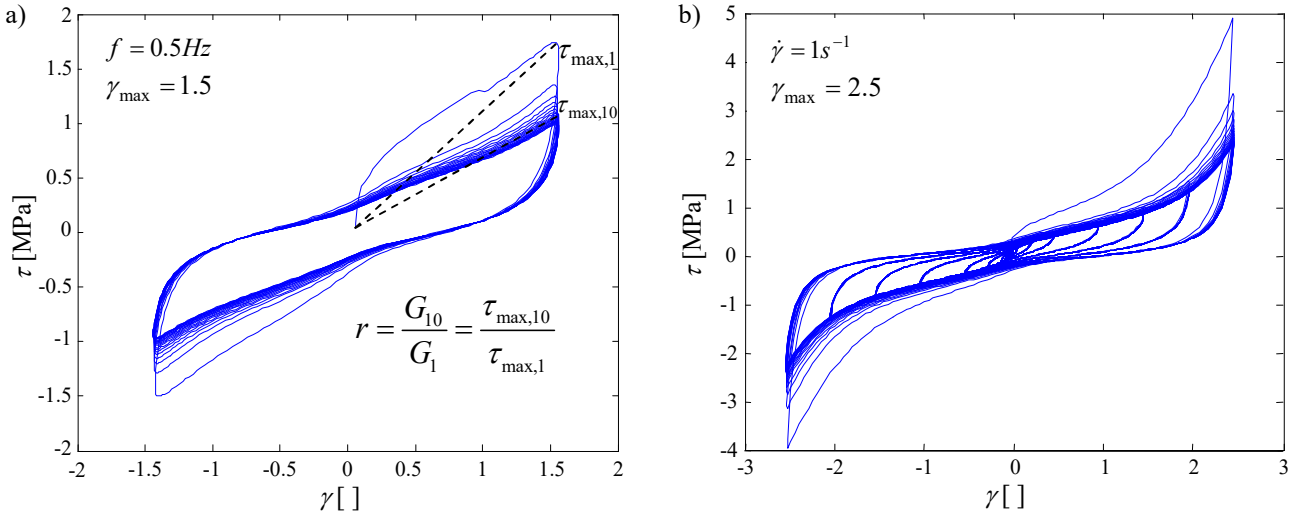

Fig. 2 – Shear tests: (a) stability under repeated cycling; (b) strain rate 1 s^{-1}.

Four further similar tests were carried out on virgin test pieces with a strain rate equal to $\dot{\gamma} = 4s^{-1}$ but for smaller values of the maximum deformation γ_{max}. In particular, values of γ_{max} equal to 2 (Fig. 3a), 1.5 (Fig. 3b), 1 (Fig. 3c) and 0.5 (Fig. 3c) were imposed. Also in this case the tests consisted of imposing 20 cycles at the maximum strain amplitude and 20 further cycles at each of the smaller amplitudes. For each of these tests, the observations made for the test with γ_{max}=2.5 are still valid. However, it is important to note that the stiffness of the stable cycles obtained at the different maximum deformations imposed are significantly different. This can be better observed in Fig. 4a where for each test only the stable cycle at the maximum strain amplitude is reported. The different stiffness of these cycles confirms that the level of softening depends on the maximum deformation experienced by the rubber. This is also confirmed by Fig. 4b, which reports the stable cycles at a small strain amplitude (0.5) for all the four tests considered. It is evident that the stiffness of these cycles decreases as the maximum strain amplitude imposed increases.

In order to investigate the strain-rate dependency of the transient response, the primary curves of the two tests carried out at $\gamma_{max} = 2.5$ and strain rates $\dot{\gamma} = 1s^{-1}$ and $\dot{\gamma} = 4s^{-1}$ are compared one to each other in Fig. 5 (a). In the same figure, the primary curves obtained with ramp tests up to $\gamma_{max} = 2.5$ and at low values of the strain rate equal to $\dot{\gamma} = 0.1s^{-1}$ and $\dot{\gamma} = 1.4 \cdot 10^{-5}$ s^{-1} (quasi-static test with execution time of about 50 hours) are reported. These tests confirm that in the range of frequencies of interest for seismic applications the dependence of the primary curves on the strain rate is not very high, though not negligible, and only at very low frequencies the stresses reduce significantly.

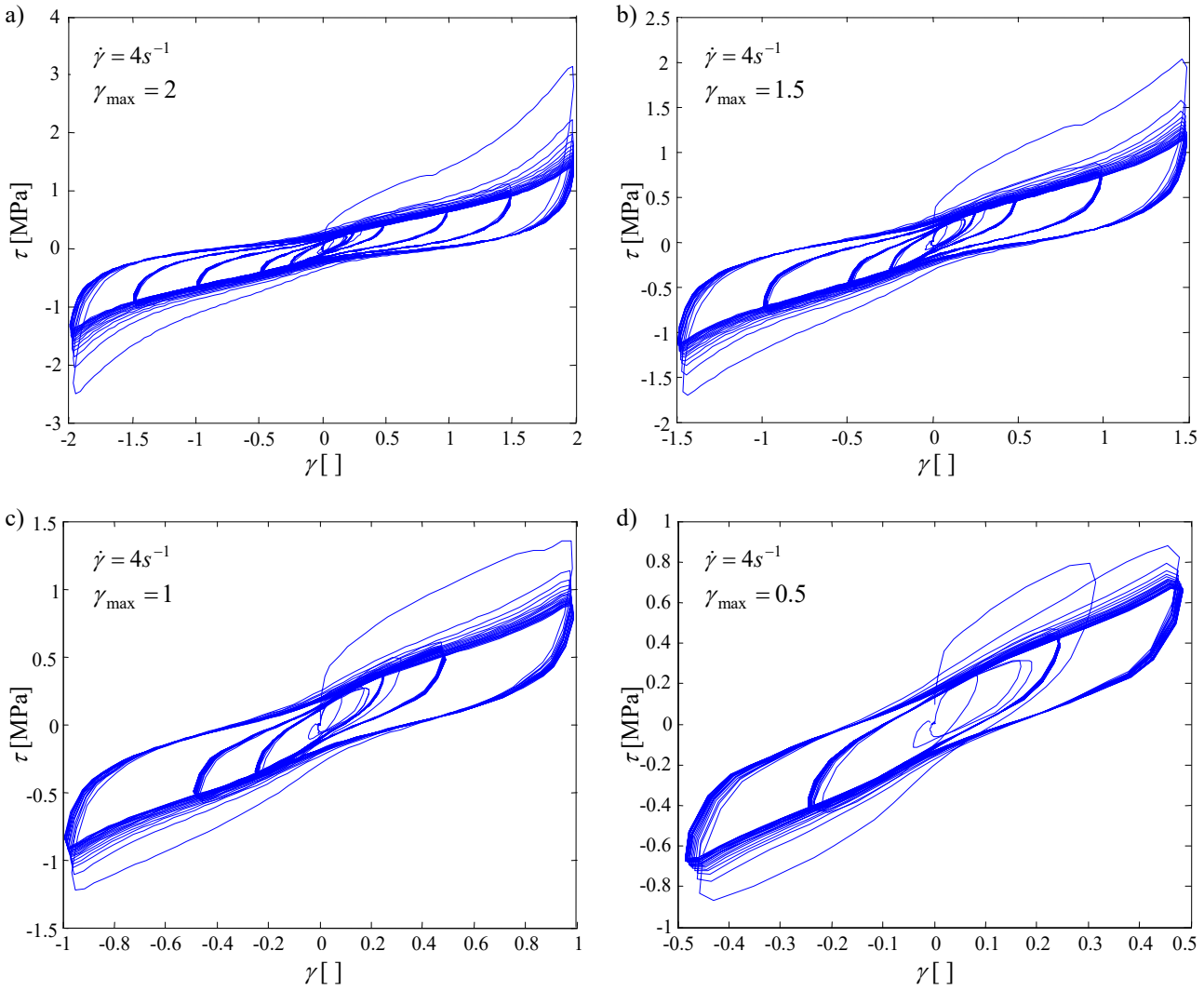

Fig. 3 – Shear tests at strain rate 4 s^{-1} corresponding to maximum shear strains of (a) 2.0; (b) 1.5; (c) 1.0; (d) 0.5.

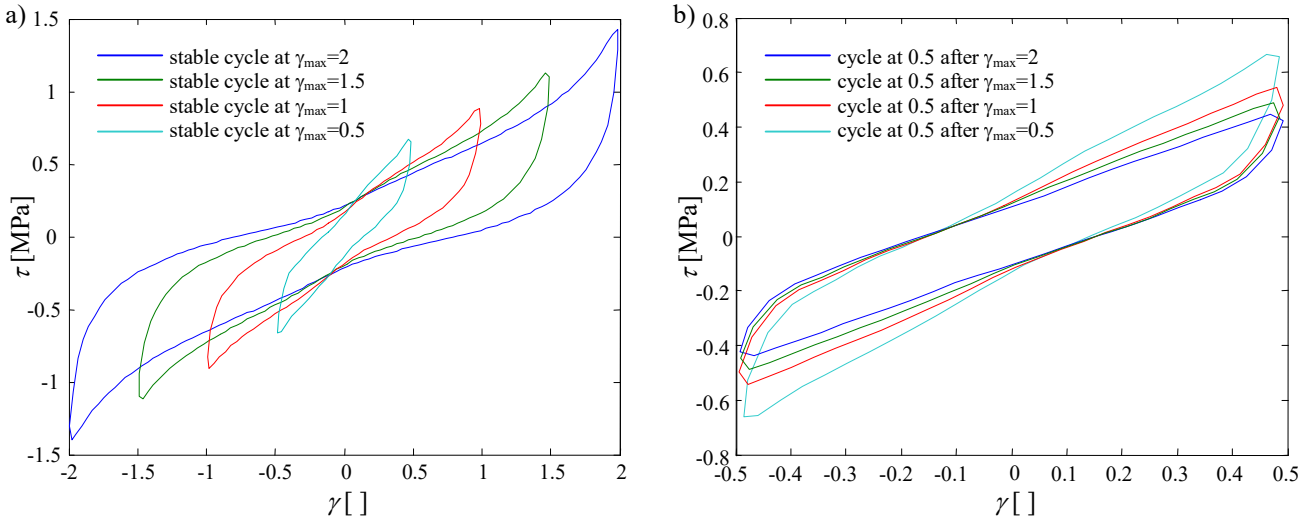

Fig. 4 –Stable cycles: (a) at different maximum strain amplitudes; (b) at a strain amplitude of 0.5 after different maximum strain amplitudes

The dependence on the strain rate of the stable cycles is also very low as can be observed in Fig. 5 (b), where the stable cycles at $\gamma_{max} = 2.5$ of the tests carried out at $\dot{\gamma} = 1s^{-1}$ and $\dot{\gamma} = 4s^{-1}$ as well as other values of the stain rate spanning from 0.1 s^{-1} to 4 s^{-1} are reported, together with the quasi-static response. The differences between the hysteretic cycles are very low and only in the loading paths

(both for positive and negative strain amplitudes) they are not negligible. However, the difference between the quasi-static response and the other responses is very significant, confirming that the material can be classified as a fading memory one, and thus it should be modelled as a viscoplastic material with long relaxation times (rather than an elasto-plastic material).
In order to further investigate this aspect and separate the elastic response from the time relaxing overstresses, multi-relaxation tests were also carried out, by imposing strain increments with rate $\dot{\gamma} = 4s^{-1}$ and by using relaxation times between each strain increment ($0.5\text{x}10^5$s) of the same order as taken to increase the strain by 1 for the quasi-static loading in Fig. 4a ($0.71\text{x}10^5$s). The stress and strain diagrams over the time are reported in Fig. 6a, confirming that the overstress contribution vanishes in a sufficient long period and that there are at least two relaxation processes leading to equilibrium with different (very short and very long) relaxation times. In Fig. 6b, the stress-strain diagram is reported, showing that the upper and lower bounds of the elastic contribution are very close. This again confirms that the rubber is a fading memory material and that after a sufficient long period of time from a seismic event the HDNR bearings return to its natural state (zero stress and zero strain) without permanent deformations.

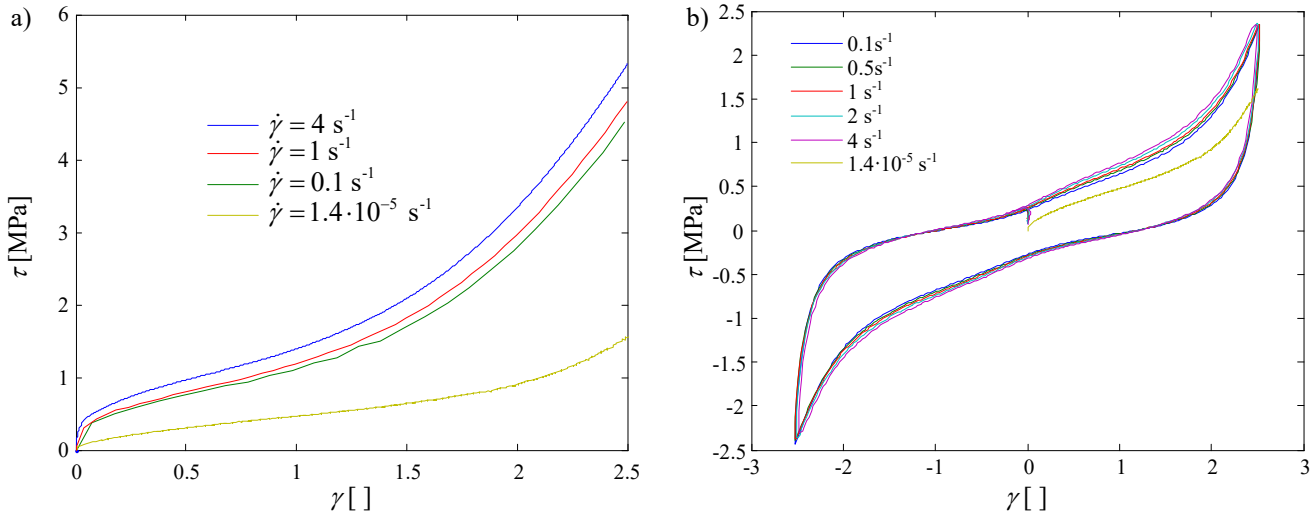

Fig. 5 – Tests with different strain rates: (a) primary curves; and (b) stable cycles at different strain rates

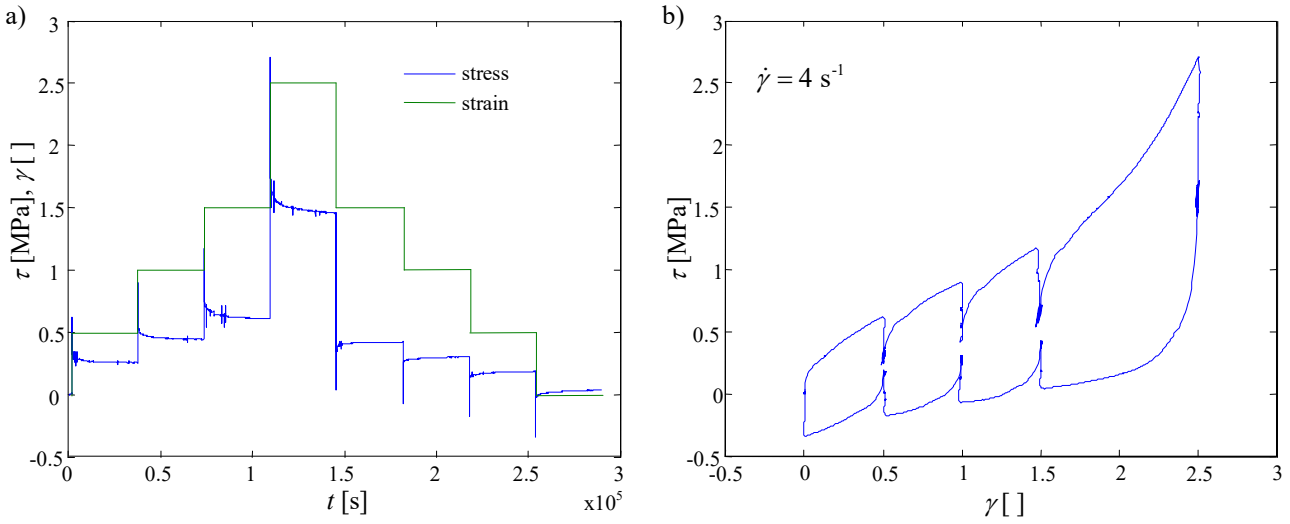

Fig. 6 – Multi-relaxation test: (a) strain and stress histories; (b) stress-strain diagram

Double shear tests for further investigation on the Mullins effect

The last parts of the experimental campaign were focused on the dependence of the Mullins effect on the shear strain direction and on the recovery properties. For the first purpose a pair of virgin

rubber samples were subjected to the strain histories reported in Fig. 7a. The first strain history consists of a common sequence of 6 full cycles with triangular shape at the amplitude 1.5 and strain rate 2 s^{-1}. The alternative history consists of 6 half cycles with triangular shape at the amplitude 1.5 followed by 6 half cycles with triangular shape at the amplitude -1.5. The hysteretic cycles corresponding to the applied strain histories are reported in Fig. 7b and confirm that the stress-softening occurring in one direction has a negligible influence on the response in the opposite direction. In fact, the maximum stress attained at negative shear strains after 6 half cycles at positive strains is very close to the stress attained in the second part of the first full cycle.

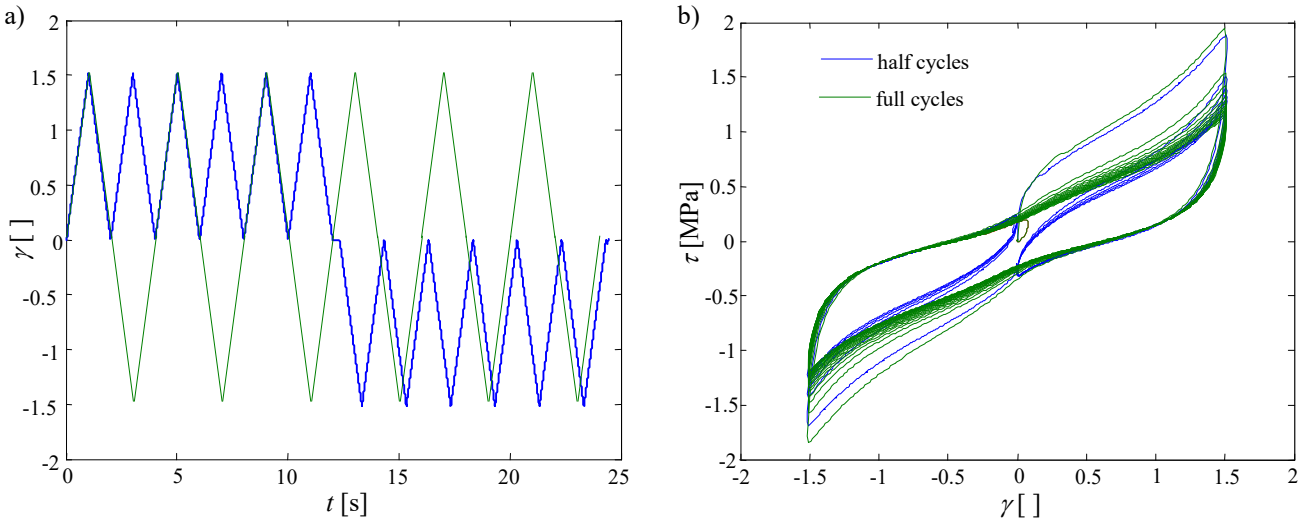

Fig. 7 – Symmetric and asymmetric tests: (a) strain histories imposed; (b) and relevant hysteretic response

Further investigations on the direction-dependence of the Mullins effect were carried out by performing a different kind of test consisting of imposing shear strains in opposite directions. In particular, the rubber has been subjected to 6 consecutive cycles in a sequence of increasing strain amplitudes along two different directions, x and y, where y is rotated by 180° with respect to x. The strain amplitudes considered for the cycles were 0.25, 0.5, 1, 1.5, and 2.5, and the rate of deformation was 2 s^{-1}. The testpiece was rested for 60 seconds between each consecutive set of 6 cycles at every amplitude and direction (which implies a partial recovery of the Mullins effect). Fig. 8 shows the imposed strain history, whereas the obtained stress-strain loops are reported in Fig. 9a.

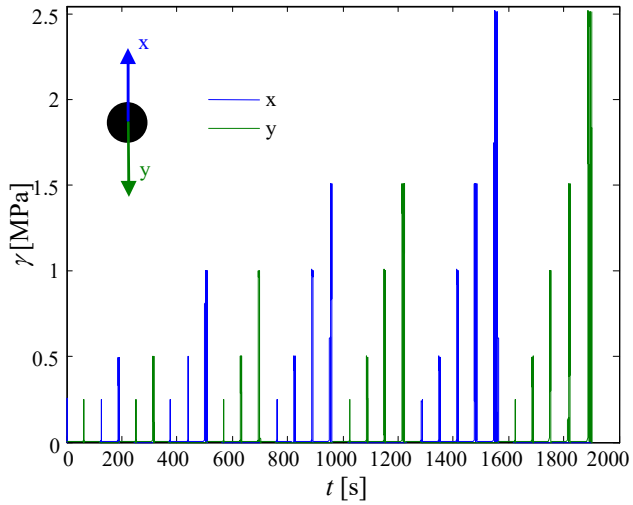

Fig. 8 – Imposed strain history of the rotated double shear test

The response in the y-direction is very close to the response in the x- direction, confirming that the Mullins effect is direction-dependent. For comparison purpose, the response to the same strain history but without rotation ($x = y$) is illustrated in Fig. 9b. It is evident that the contribution of the

Mullins effect is reduced when repeating the tests in the same direction, though it is not negligible due to the recovery occurring between each test sequence.
Finally, the recovery properties after a sufficient long period of time are investigated. To this purpose, a test at maximum strain amplitude $\gamma_{max} = 2.5$ and rate $\dot{\gamma} = 4s^{-1}$ was performed on a sample previously tested at the same maximum amplitude after a period of rest of 6 months and results are compared with the primary curve related to the same strain rate. The comparison is shown in Fig. 10, where it can be observed that the primary curve of the test repeated after 6 month is very close to the primary loading curve of the virgin rubber, even if some differences can be observed especially at small strain amplitudes. This confirms that the Mullins effect is a reversible phenomenon for this HDNR compound, i.e. it has recovered most of its initial properties after 6 months rest.

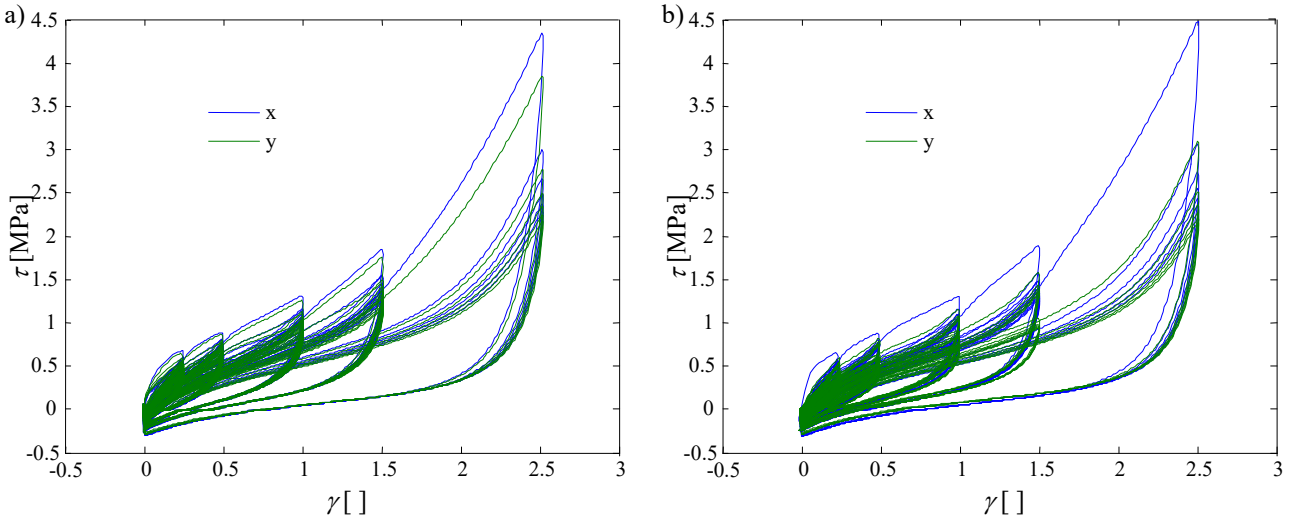

Fig. 9 – Stress-strain cycles: (a) rotated and (b) not rotated double shear test

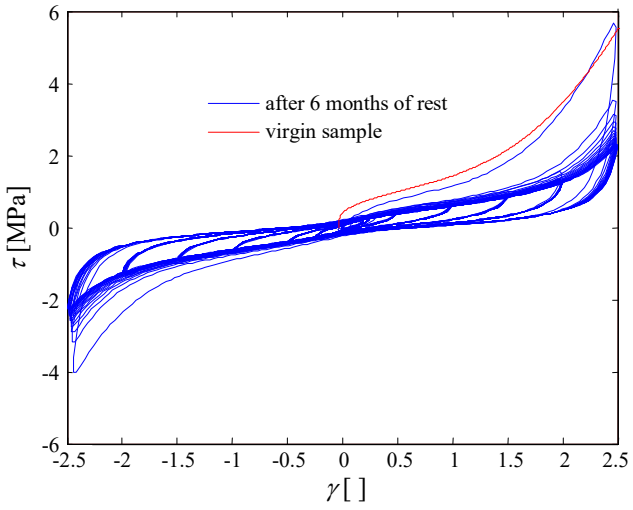

Fig. 10 – Mullins effect recovery

HDNR CONSTITUTIVE MODEL

This section describes a one-dimensional constitutive model for HDNR in simple shear accounting for the strain-path history dependent phenomena observed in the experimental test results presented in the previous section. The proposed model introduces several advances in the description of the stress-softening behaviour of rubber. In fact, while several analytical models are available in the technical literature that allow an accurate simulation of the stable HDNR bearing behaviour, few models are able to describe the transient softening response and none of these models account for the direction dependence of the Mullins effect. The proposed model is tested not only against the

experimental data above, but also with respect to two additional double shear tests, to compare simulation and experiment for strain histories representative of earthquakes, before and after scragging.

Models overview and proposed model

The proposed model provides a relation between the shear strain γ and the shear stress τ, from which the bearing force-displacement relationship can be evaluated through simple geometrical considerations. In particular, the stress-strain material response is decomposed into two contributions:

$$\tau = \tau_0 + \tau_m \tag{1}$$

where the former (τ_0) is the stable component not affected by the strain history, whereas the latter (τ_m) describes the additional transient response, which degenerates as the stress-softening evolves during the strain history.

Similarly to Dall'Asta and Ragni [22], the component τ_0 of the stress is described by assuming a rheological model consisting of a nonlinear elastic spring, modelling the non linear stiffening behaviour of the rubber at large strains, acting in parallel with two rate-dependent elements, modelling the dissipative component of the response [19-24]. It can be expressed in the form:

$$\tau_0 = \tau_e(\gamma) + \tau_{v1}(\gamma, \dot{\gamma}, \dot{\gamma}_{v1}) + \tau_{v2}(\gamma, \dot{\gamma}, \dot{\gamma}_{v2}) \tag{2}$$

where:

$$\tau_e(\gamma) = a\gamma^5 + b\gamma^3 + c\gamma \tag{3}$$

represents the nonlinear elastic contribution which still exists once all the overstresses are relaxed (see Fig. 6b). The other terms describe the over-stresses relaxing in time. At least two terms are required to describe different material behaviours: the term τ_{v1}, representing the main dissipative contribution of the response not sensitive to strain rates typical of seismic histories (but sensitive to very low strain rates as showed by the tests at strain rate equal to $1.4 \cdot 10^{-5}$ s^{-1} reported in Fig.5b), and the term τ_{v2}, which is a visco-elastic term sensitive to strain rates typical of seismic histories, but very low for the rubber considered in this paper (see Fig. 5b). Different approaches can be found in the technical literature for modelling the main dissipative contribution. In [22], a rate-dependent viscous-plastic model was used, based on the plastic model originally proposed by Ozdemir [37]. Differently, rate independent hysteretic models based on different formulations were adopted by other authors [19-21,23-24]. Among these rate-independent models, the model proposed in Huang [38] and later extended in Grant et al. [24-25] on the basis of the Bounding Surface (BS) theory, firstly developed by Dafalias and Popov [39], is particularly convenient for the HDNR behaviour simulation, since it enables more accurate description of the change of stiffness with the strain amplitude for both loading and unloading paths. In particular, in Grant [24-25] a BS model with a vanishing elastic region depending on the current value of shear strain was adopted to better match the tests. In this paper, a modified BS model with vanishing elastic region is also proposed to describe the main dissipative contribution τ_{v1}. In particular, based on the experimental results, the modifications described in the following are introduced. First of all, a dashpot is considered in series with the BS model, in order to maintain the relaxation property of the model. As a consequence of this assumption and the elastic region being vanishing, the plastic shear strain γ_p is the difference between the total shear strain γ and the inelastic strain γ_{v1}, whose rate is controlled by the following evolution law

$$\dot{\gamma}_{v1} = \nu_1 \tau_{v1} \tag{4}$$

The stress is provided by an incremental law, where the shear stress rate $\dot{\tau}_{v1}$ is obtain from the plastic shear strain rate $\dot{\gamma}_p = (\dot{\gamma} - \dot{\gamma}_{v1})$ through the relation:

$$\dot{\tau}_{v1} = E_p \dot{\gamma}_p \tag{5}$$

The parameter E_p is the varying plastic modulus describing the non linear behaviour of the rubber from the yielding surface (vanishing in this case) to the bounding surface (R) . It can be written as:

$$R = \xi_0 + \xi_1 \gamma_p^2 \tag{6}$$

The expression for the plastic modulus may have many different forms [24,39,40]. In this paper, one similar to Grant et al. [24] is used:

$$E_p = E_{p0}(\gamma) + \xi_2 \delta = \frac{dR}{d\gamma_p} sign(\dot{\gamma}_p) + \xi_2 \delta = 2\xi_1 \gamma_p sign(\dot{\gamma}_p) + \xi_2 \delta \tag{7}$$

where $E_{p0}(\gamma)$ is the value of the plastic modulus when the yield surface and boundary surface intersect, while δ is the positive difference between the current stress and the appropriate bounding surface $R \cdot sign(\dot{\gamma}_p)$, being positive in loading processes (when $\dot{\gamma}$>0) and negative in unloading processes (when $\dot{\gamma}$<0), as expressed by the following equation:

$$\delta = \left| R \cdot sign(\dot{\gamma}_p) - \tau_{v1} \right| \tag{8}$$

According to Equation (7), the plastic modulus becomes infinite when δ tends to infinity. However, differently from [24] and in order to better fit the experimental results, it is assumed that the parameter ξ_2 controlling the dependence of the plastic modulus on the distance δ linearly depends on the magnitude of the current plastic deformation, according to the following expression:

$$\xi_2 = \xi_{2,1} + \xi_{2,2} \left| \gamma_p \right| \tag{9}$$

Finally, for the viscous term τ_{v2}, due to its very low contribution to the global behaviour for the rubber considered, a simple Maxwell element is adopted:

$$\tau_{v2}(\gamma, \gamma_{v2}) = E_{v2}(\gamma - \gamma_{v2}) \tag{10}$$

The internal variable γ_{v2} describes the inelastic strain and its evolution is given by the law:

$$\dot{\gamma}_{v2} = \nu_2 \tau_{v2}(\gamma, \gamma_{v2}) \tag{11}$$

where the relaxation time is $1/(\nu_2 E_2)$. The material parameters adopted for the model have been calibrated based on the results of the tests. More specifically, the elastic contribution has been fitted first by considering the multi-relaxation test results of Fig. 6. Once the elastic contribution is identified, the parameters related to the main dissipative contribution have been determined on the basis of the stable cycles of the test results reported in Fig. 2b. Finally, the parameters of the visco-elastic contribution have been calibrated by considering the stable cycles with different strain rates reported in Fig. 5. Table 1 reports the values obtained for the parameters.

Table 1 – Model parameters of the stable (left) and transient (right) response

τ_e			τ_{v1}					τ_{v2}		τ_{me}			τ_{mv}		
a	b	c	ξ_0	ξ_1	$\xi_{2,1}$	$\xi_{2,2}$	ν_1	E_2	ν_2	α_e	ξ_e	β	α_v	ξ_v	β
MPa	MPa	MPa	MPa	MPa	-	-	$MPa^{-1}s^{-1}$	MPa	$MPa^{-1}s^{-1}$	-	-	-	-	-	-
0.015	-0.05	0.28	0.14	0.08	3.5	1.5	0.4	0.068	8.5	1.7	0.25	0.4	2.2	0.13	0.4

In Fig. 11 the elastic contribution (Fig. 11a) and the two dissipative contributions (Fig.11b) are shown separately for the test described in Fig. 2.

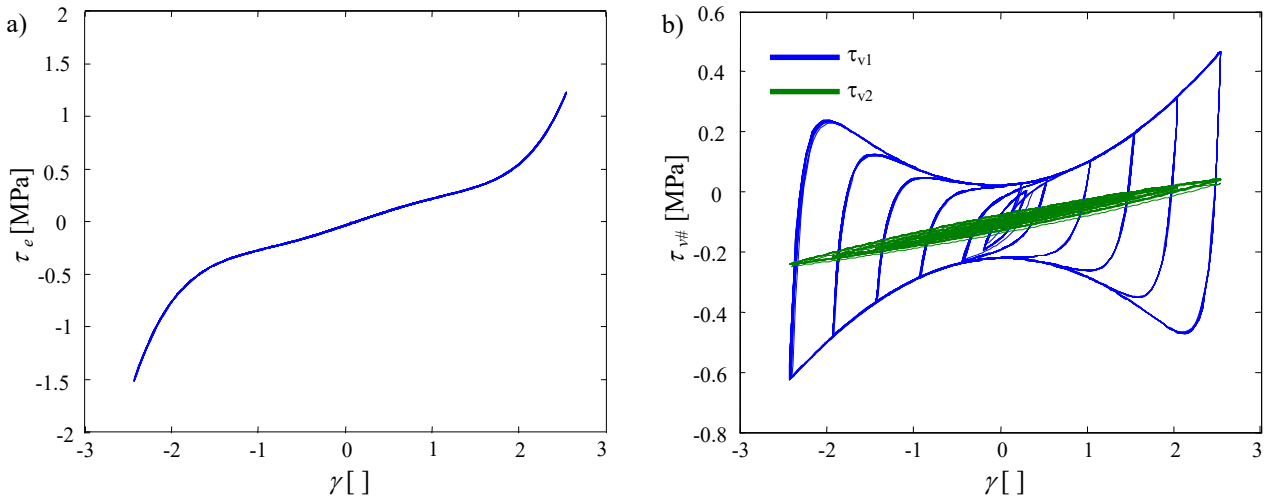

Fig. 11 – Contributions for the test described in Fig. 2b: (a) elastic; (b) dissipative

The stress-softening behaviour of the rubber response is usually described through damage models [20,22,24] and the key point is in the definition of the laws describing the damage evolution. The model proposed in this paper recovers some basic ideas already proposed in Dall'Asta and Ragni [22], such as the use of different damage parameters and the dependence of the damage limits on the current strain, but it is based on a new set of damage parameters and associated evolution laws that better describe the response observed in the tests. In particular, the tests reported in Fig. 2 and 3 show that the major effect is progressive reduction of the stiffness as the strain history progresses and that the material tends to different stable loops for different maximum strains experienced by the rubber. This phenomenon can be described by means of a damage parameter q_e affecting the elastic response (τ_e) and which progressively grows towards a limit value which varies with the current total strain. However, in order to account for the direction dependence of the stress-softening, as highlighted by the experimental results reported in Figs. 7 and 9, two separate damage parameters q_e^+ and q_e^- evolving only for positive and negative strains respectively are introduced. A minor softening effect concerns the reduction of the cycle amplitude at zero strain, as measured by the stress intercept. This latter effect cannot be related to an elastic contribution, which is null for zero strains, thus the response reduction is due to a further softening mechanism, described by the parameter q_v involving the dissipative response (τ_{v1} and τ_{v2}). Note that the direction dependence of the softening relates to the elastic contribution only and cannot be assumed for q_v, because this would lead to discontinuities in the shear stress by passing from positive to negative strains which are not observed in the tests. Thus, this parameter evolves both for positive and negative strains so that the response in the negative direction is slightly affected by cycling at the positive direction, as observed in the experiments. Assuming that the initial response is proportional to the stable one, the stress-softening response can be written as:

$$\tau_m = \tau_{me} + \tau_{mv} \tag{12}$$

where the damage contribution affecting the elastic response (τ_{me}) along the two directions and the one affecting the dissipative response (τ_{mv}) can be expressed as:

$$\tau_{me} = \alpha_e \left(1 - q_e^+\right) \tau_e \text{ for } \gamma > 0 \tag{13a}$$

$$\tau_{me} = \alpha_e \left(1 - q_e^-\right) \tau_e \text{ for } \gamma < 0 \tag{13b}$$

$$\tau_{mv} = \alpha_v \left(1 - q_v\right) \left(\tau_{v1} + \tau_{v2}\right) \tag{13c}$$

For all the damage parameters it is assumed that their evolution is proportional to the strain rate, i.e. they evolve as the strain history progresses, and that their limit value depends on the current value of strain. In particular, the evolution laws of the elastic damage parameters for $\gamma > 0$ are posed in the following form:

$$\dot{q}_e^- = 0 \qquad (14a)$$

$$\dot{q}_e^+ = \zeta_e |\dot{\gamma}| \left(\left(\frac{\gamma}{\gamma_{\text{mod}}} \right)^\beta - q_e^+ \right) \qquad \text{if} \quad q_e^+ < \left(\frac{\gamma}{\gamma_{\text{mod}}} \right)^\beta \qquad (14b)$$

$$\dot{q}_e^+ = 0 \qquad \text{if} \quad q_e^+ \geq \left(\frac{\gamma}{\gamma_{\text{mod}}} \right)^\beta \qquad (14c)$$

For $\gamma < 0$ the roles of $\dot{q}_e^+$ and $\dot{q}_e^-$ are interchanged in equations 14 and γ is replaced by $|\gamma|$. During a cyclic strain history both the damage parameters q_e^+ and q_e^- tend to the same limit value, depending on the amplitude of the strain cycle and the velocity of the damage evolution is controlled by the parameter ζ_e. In particular, the maximum value that can be reached by q_e^+ and q_e^- for strain amplitudes not exceeding $|\gamma|$ is given by the expression $(|\gamma|/\gamma_{\text{mod}})^\beta$ where γ_{mod} is the maximum amplitude for which the model is deemed valid (γ_{mod}=2.5 for this model). It should be noted that Eqn. 14b ensures that the damage parameters cannot decrease and that they do not increase further once their limit depending on the current strain has been attained. Finally, for the damage parameter q_v a similar evolution law is assumed, with the same maximum values as for q_e^+ and $\dot{q}_e^-$ but with a different velocity parameter (ζ_v) and without the strain-direction dependency:

$$\dot{q}_v = \zeta_v |\dot{\gamma}| \left(\left(\frac{|\gamma|}{2.5} \right)^\beta - q_e^+ \right) \qquad \text{if} \quad q_v < \left(\frac{|\gamma|}{\gamma_{\text{mod}}} \right)^\beta \qquad (15a)$$

$$\dot{q}_v = 0 \qquad \text{if} \quad q_v \geq \left(\frac{|\gamma|}{\gamma_{\text{mod}}} \right)^\beta \qquad (15b)$$

The values of the material parameters adopted for describing the stress-softening, based on fitting to the experimental test results of Figs. 2b, 3 and 7, are given in Table 1. Fig. 12 shows the two contributions of the transient response for the test described in Fig. 2b.

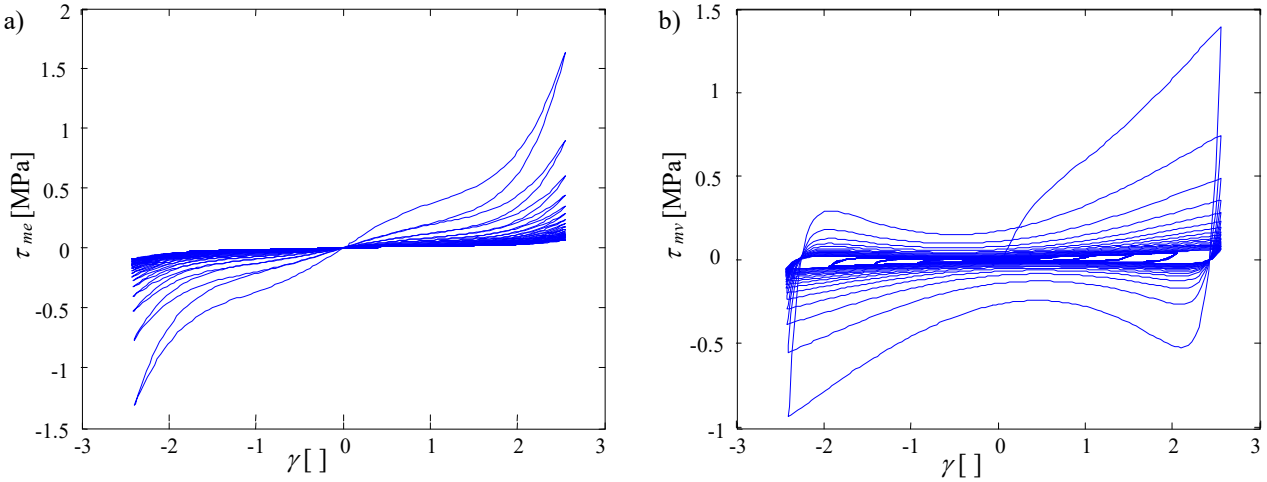

Fig. 12 –Softening contributions for the test described in Fig. 2b: (a) τ_{me} affecting the elastic response ; (b) τ_{mv} affecting the dissipative response.

Numerical simulation of the tests

The test described in Fig. 7 and consisting of cycles with positive strains followed by cycles with negative strains is firstly simulated to show the ability of the proposed model to describe the direction-dependence of the Mullins effect. Fig. 13a compares the hysteretic loops obtained by testing and by simulation, whereas Fig. 13b shows the evolution with cycling of the three damage parameters of the model up to the limit corresponding to the maximum strain amplitude of 1.5. Fig. 14a compares the experimental and numerical hysteretic responses corresponding to the test of Fig. 2b, whereas Fig. 14b the evolution of the damage parameters of the transient response according to the numerical model.

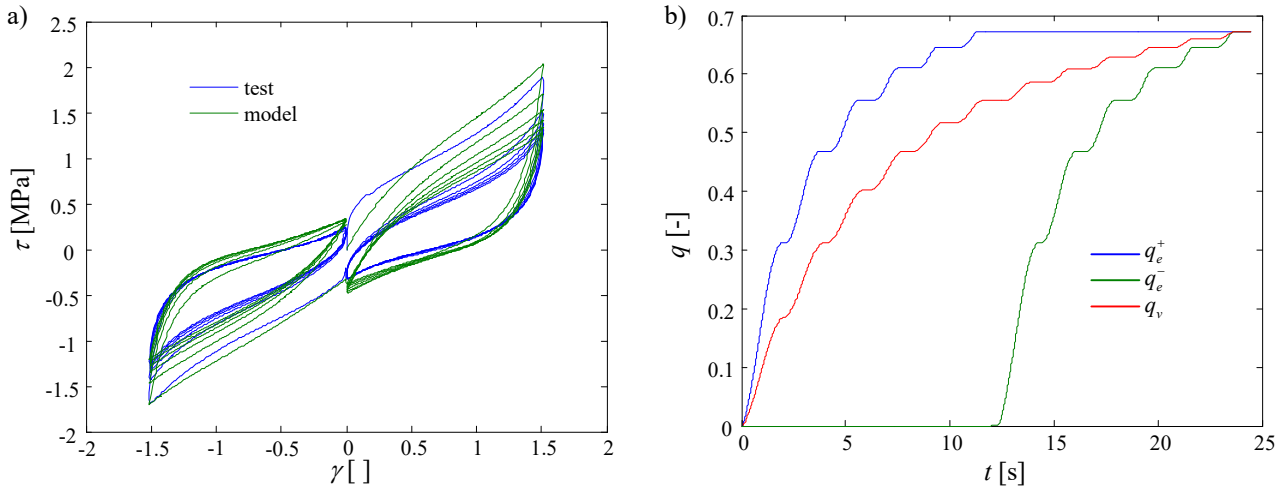

Fig. 13 – (a) Simulation of the asymmetric test of Fig. 7 half cycle tests; (b) evolution of damage parameters

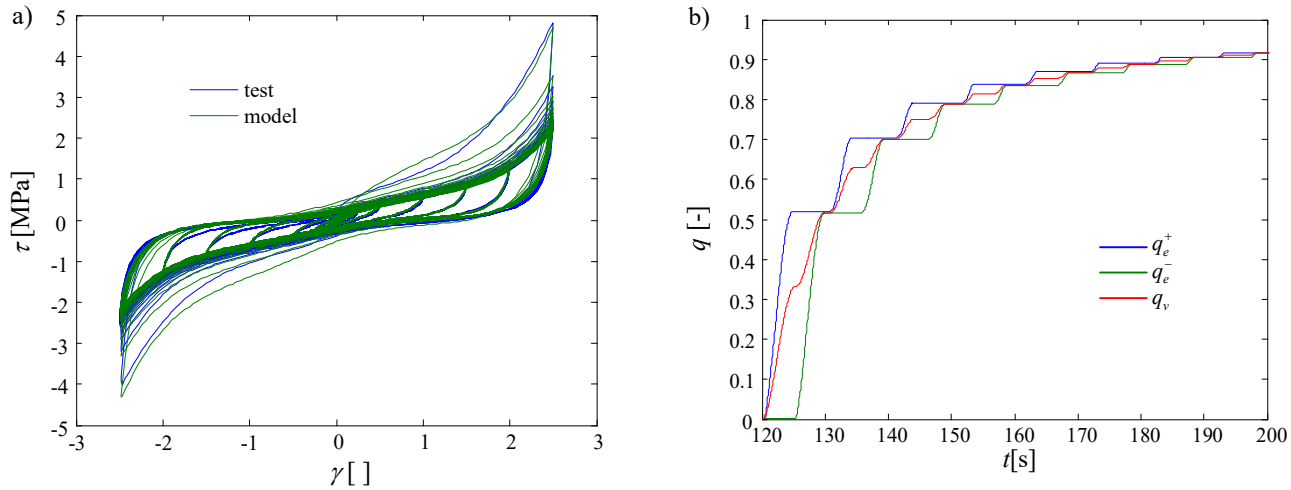

Fig. 14 – (a) Simulation of the test at strain rate $1s^{-1}$ of Fig. 2b; (b) evolution of damage parameters

Fig. 15 reports the results of the simulation of the tests described in Fig. 3. In all the cases, the agreement between experimental and numerical results is very satisfactory. Thus, the ability of the model to predict the near-stable and transient response of the rubber at different strain rates and strain amplitudes is verified, also for very small strain amplitudes (Fig. 15c,d).

Finally, the ability of the model to simulate the seismic response of isolated structures has been checked by performing two further tests in which the strain histories reported in Fig. 16 have been imposed. These imposed strain histories represent the simulated displacement responses of a S-DOF isolated structure under a near-fault (Fig. 16a) and a far-field (Fig. 16b) record prior to and after scragging cycles consisting of ten cycles at 0.5 Hz with 250% shear strain, as can be seen in Fig. 16. The strain history before the application of scragging is used to test the capability of the HDNR model to simulate the behaviour of the rubber in the virgin isolators, whereas the strain history after the scragging procedure is used for validating the model for simulation of the scragged behaviour.

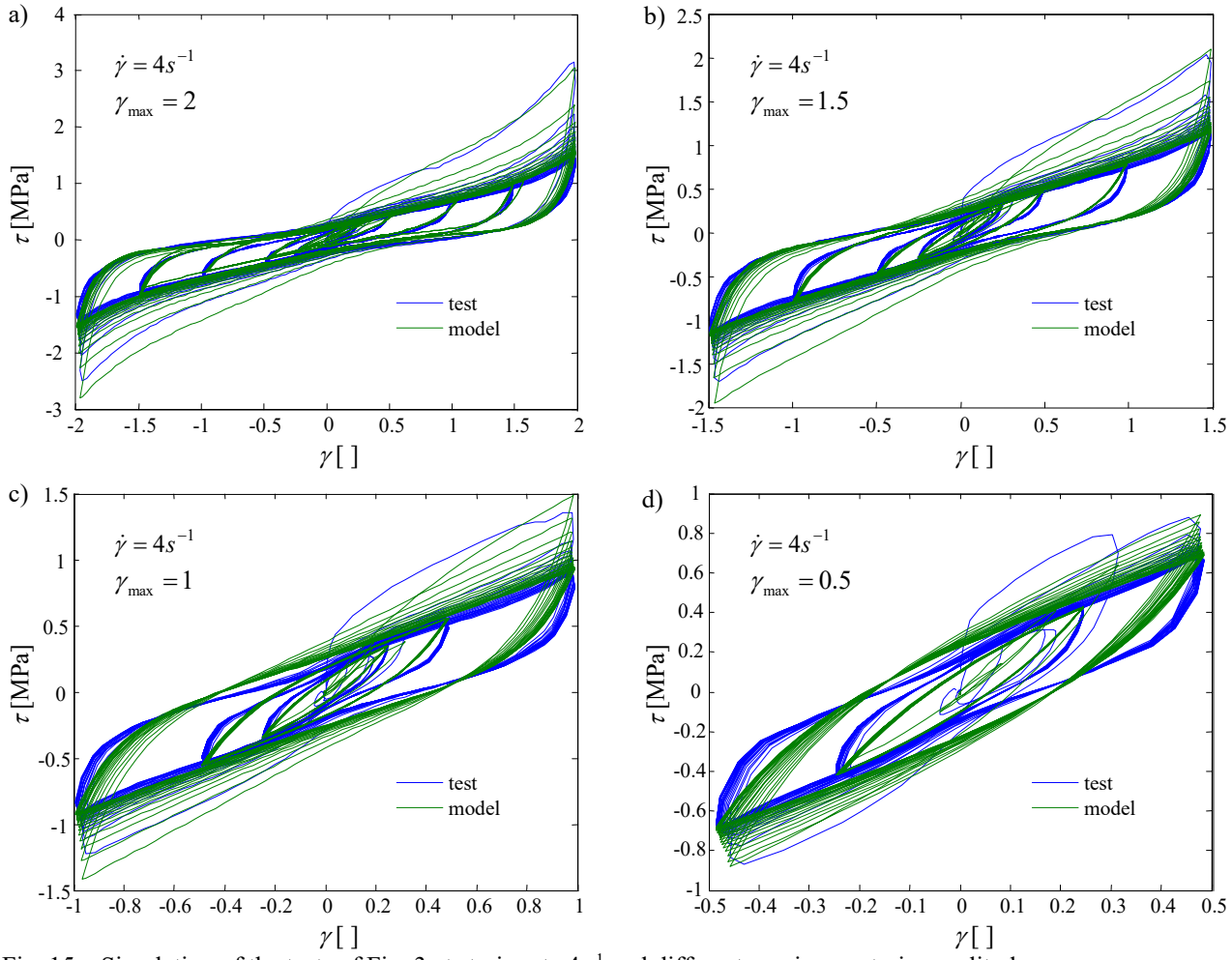

Fig. 15 – Simulation of the tests of Fig. 3 at strain rate $4s^{-1}$ and different maximum strain amplitudes

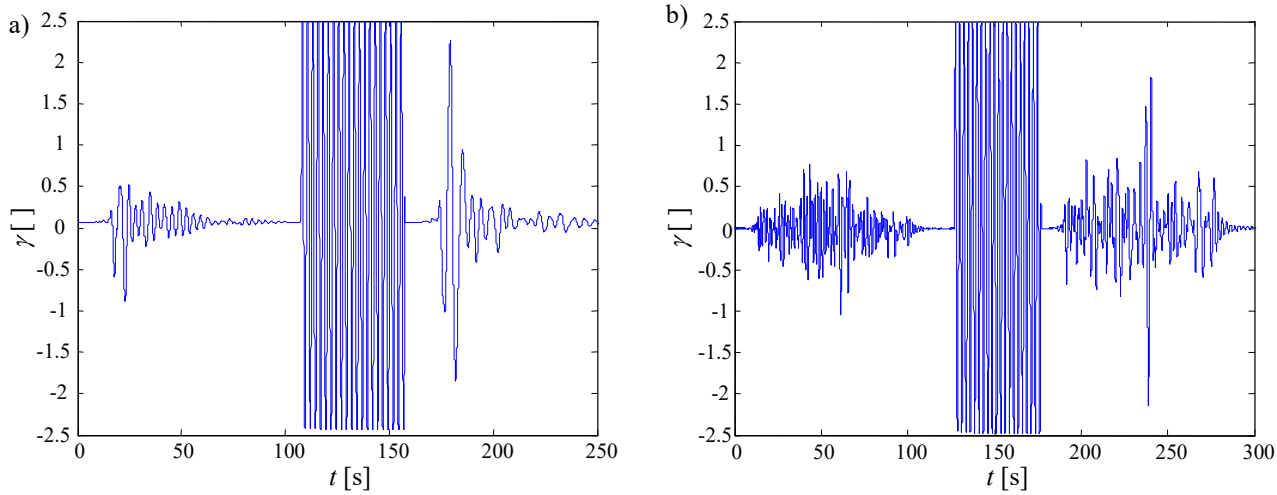

Fig. 16 – Imposed strain histories simulating the response under seismic excitations before and after a scragging procedure: (a) near fault record (Northridge-0-Newhall-W Pico Canyon station); (b) far-field record (Imperial Valley-06-Delta station)

Fig. 17 compares the experimental and numerical responses obtained under the near-fault record (Figs. 17a,b) and the far-field record (Figs. 17c,d) respectively in the virgin and scragged conditions. In all the cases, good agreement between the experimental and numerical response is obtained.

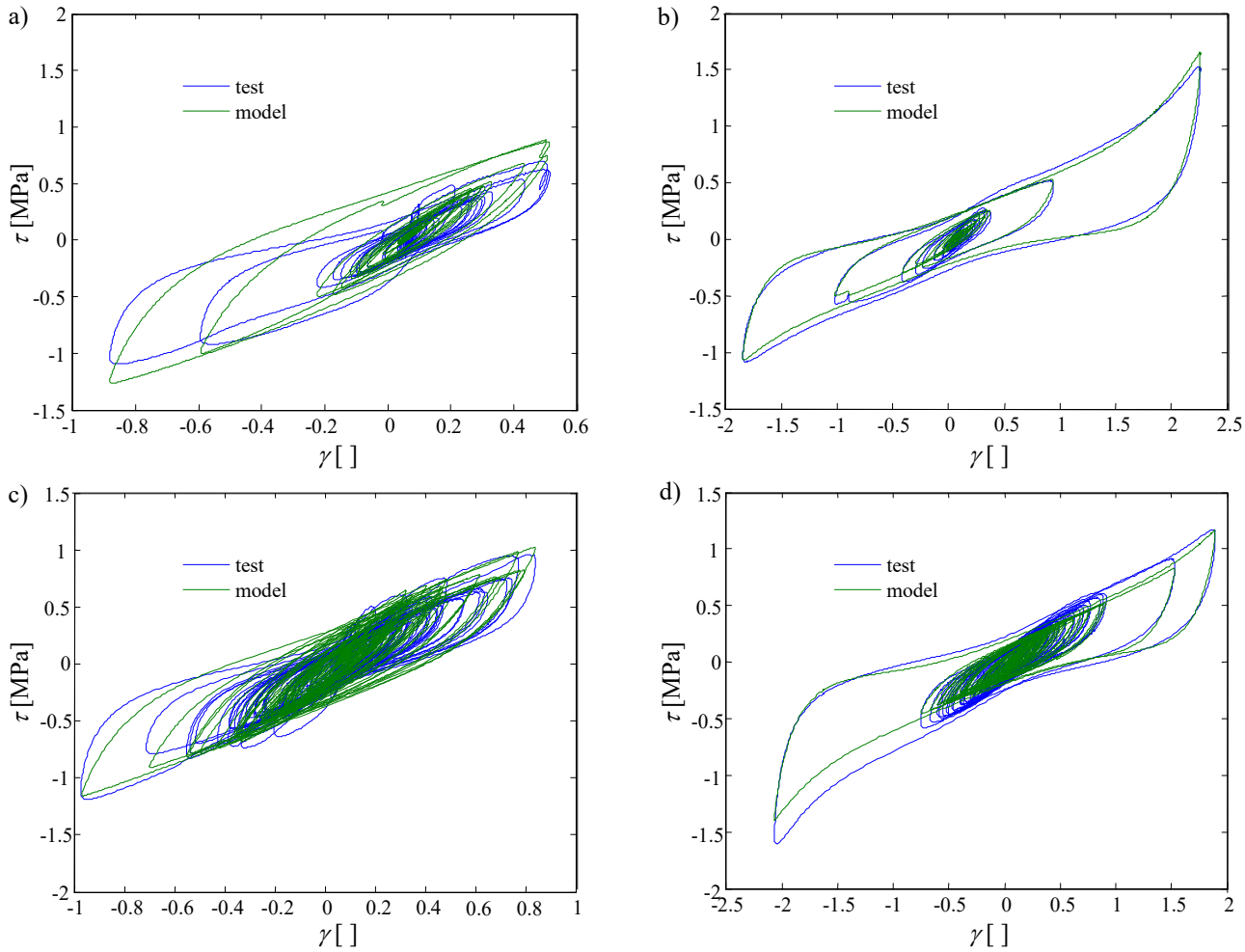

Fig. 17 – Stress-strain simulations for the seismic response excitations of Figure 16: (a) near fault prior to scragging; (b) near-fault after scragging; (c) far-field prior to scragging; (d) far-field. after scragging .

SEISMIC RESPONSE

In this section, the proposed rubber model is employed to simulate the horizontal response under the design conditions (far from the collapse) of virgin laminated HDNR bearings with shape factors used in the design practice [16,17], so that the hypothesis of uniform simple shear is realistic. In particular, numerical analyses aim at evaluating the influence of the stress softening on the predicted seismic response of isolated structures. To this purpose, a simplified isolated structure modelled as a S-DOF system is considered and the process-dependent response has been studied by performing two different sets of dynamic analyses under seismic events with different duration and frequency content. More precisely, the case of near-fault (NF) ground motions and the case of far-field (FF) ground motions are separately studied. To highlight the contribution of the stress-softening, the solution provided by the proposed model for the virgin material is compared with the solution evaluated by using a "scragged" model, where the softening corresponding to the design strain amplitude is fully developed. It is noteworthy that this latter condition may not occur during the lifetime of the isolated structure, because of the recovery properties of the Mullins effect and the long time between earthquakes of significant intensity. However, the kinetics of recovery have so far not been thoroughly investigated, nor does the numerical model as yet account for any recovery of the Mullins effect. The comparison given here permits to investigate and evaluate the highest possible effects of the stress-softening on the seismic response of structures isolated with HDNR.

Case study and seismic response evaluation

The case study consists of an isolated structure modelled as a S-DOF system, with a mass M=800 kNs^2/m which is assumed representative of that of a realistic multistorey building. For the isolation system, a rubber thickness equal to t_r=0.138 m is assumed in order to have a maximum shear strain equal to 1.5 under a realistic value of the maximum displacement equal to 0.2m. The isolation system is finally defined by the total rubber area, which is assumed equal to A=0.917 m^2. For example, a number of 6 isolators may be assumed, with diameter D=450mm and total rubber thickness arranged in 28 layers of thickness t about 5mm (corresponding to S_1=D/4t=22.5 and S_2=D/t_r=3.2). The total stiffness of the isolation systems can be estimated by K_{is}=GA/t_r, where G=1.18 N/mm^2 is the shear modulus evaluated as the average over three cycles [35] of a numerical sinusoidal test carried out at the design shear amplitude and frequency. The relevant vibration period of the isolated structure is about T_{is}=2 s.
The load-history dependent behaviour of the virgin isolation system is described by the model introduced in the previous section and several ground motions are considered to evaluate the effects due to the load-history dependence. In particular, two sets of ground motion records are considered, one representative of far field (FF) and the other of near-fault (NF) seismic inputs. Considering that FF and NF have strongly different time histories and frequency contents, response with different characteristics are expected, thus the two cases are studied separately. General information about the records employed and the relevant scale factors are reported in Tables 2 and 3. Table 3 also reports the period T_p of the dominant pulses of the NF records. It can be observed that the pulse periods are higher than the design isolation period (T_{is}=2s). Moreover, scale factors for NF records are all lower than 1 and in general smaller scale factors are required for T_p values close to T_{is} while higher scale factors are required for T_p values much higher than T_{is} and away from resonance [41,42].

Table 2. Far-field ground motions.

Name	Event	Station	Magnitude	Rrup(km)	Component	PGA (g)	SF
FF1	Northridge-01	Beverly Hills-12520 Mulhol	6.69	18.36	H1	0.535	1.87
FF2	Northridge-01	Beverly Hills-14145 Mulhol	6.69	17.15	H1	0.440	0.80
FF3	Northridge-01	Castaic - Old Ridge Route	6.69	20.72	H1	0.505	1.19
FF4	Imperial Valley-06	Delta	6.53	22.03	H1	0.262	1.47
FF5	Imperial Valley-06	Delta	6.53	22.03	H2	0.262	1.26
FF6	Imperial Valley-06	El Centro Array #13	6.53	21.98	H1	0.118	3.65
FF7	Imperial Valley-06	Niland Fire Station	6.53	36.92	H1	0.088	5.32

Rrup= Closest distance to rupture plane, H # =component name, SF =scale factor

Table 3. Near-fault ground motions.

Name	Event	Station	Magnitude	Rrup(km)	Comp.-T_p(s)	PGA(g)	SF
NF1	Northridge-01	Sylmar-Converter Sta	6.69	5.35	FN - 3.5	0.698	0.50
NF2	Northridge-01	Sylmar-Converter Sta East	6.69	5.19	FN - 3.5	0.686	0.68
NF3	Landers	Lucerne	7.28	2.19	FN - 5.1	0.727	0.60
NF4	Northridge-01	Newhall - W Pico Canyon	6.69	5.48	FN - 2.4	0.363	0.45
NF5	Imperial Valley-06	El Centro Array #6	6.53	1.35	FN - 3.8	0.448	0.66
NF6	Imperial Valley-06	El Centro Array #6	6.53	1.35	FP - 2.6	0.448	0.78
NF7	Imperial Valley-06	El Centro Array #7	6.53	0.56	FN - 4.2	0.437	0.72

Rrup= Closest distance to rupture plane, FN=fault normal component NP= fault parallel component, SF =scale factor
T_p = pulse period

In order to compare results for different seismic inputs, the selected ground motions are scaled to provide a maximum value of displacement equal to 0.2m in the model with the "virgin" HDNR bearings, corresponding to the design strain amplitude γ_{is} =1.5. For each analysis, in addition to the “virgin” case, also the "scragged" case is considered. For the latter case the assumption is that the stress-softening effect has fully exhausted at the design strain amplitude γ_{is}=1.5. This condition,

from Eqs.14-15, corresponds to an initial value of the damage parameters equal to the limit value at the design strain amplitude, i.e. $(1.5/2.5)^{0.4}=0.82$, evolving only if the strain amplitude 1.5 is exceeded. In this way, the effects of the stress-softening can be effectively quantified under different path histories producing the same maximum strain amplitude in the virgin case.

Table 4 reports the results of all the time-history analyses in terms of peak values of bearing shear strain γ_b and bearing shear stress τ_b obtained by considering the virgin and the scragged bearing properties, for both the FF and NF records. First of all, note that the results related to the virgin case confirm that the virgin behaviour of bearings is significantly influenced by the displacement-history dependent softening process. In fact, although in all the analyses the maximum shear strain is equal to 1.5, the corresponding shear stresses are quite different. In particular, the maximum shear stresses obtained for the FF records range from 1.54 MPa, when the softening during the excitation is greatest, to 2.04 MPa, when the softening is least. The highest values of maximum stress correspond to response histories characterized by few small-amplitude cycles taking place before the largest one, whereas the lowest values correspond to histories with several cycles taking place before the largest one. The responses to record FF2 and to record FF5 are representative of these two cases, as can be seen in the plots of the hysteretic response of the virgin rubber (green lines in Fig.s 18a and 18b) and of the evolution of the three damage parameters for these records (Fig.s 18c and 18d). Differently, in the case of NF records, the response histories are all characterized by few small-amplitude cycles before the largest one, thus the values of the shear stresses are all high and similar to each other (from 1.82 MPa to 2.08 MPa). This trend can also be observed in Fig.s 19a and 19b, plotting the shear stress-strain diagram relevant to two NF records (NF3 and NF6), and Figs. 19c and 19d, reporting the relevant evolution of the damage parameters of the HDNR model.

Table 4. Peak response values for FF and NF ground motions.

FF records					NF records				
	γ_b [-]		τ_b [MPa]			γ_b [-]		τ_b [MPa]	
acc.	virgin	scragged	virgin	scragged	acc.	virgin	scragged	virgin	scragged
FF1	1.500	1.365	1.924	0.972	NF1	1.500	2.529	1.815	2.859
FF2	1.500	1.334	1.896	0.946	NF2	1.500	2.072	2.075	1.767
FF3	1.500	1.429	2.044	0.994	NF3	1.500	2.221	2.038	2.067
FF4	1.500	2.049	1.543	1.691	NF4	1.500	2.324	2.056	2.342
FF5	1.500	1.696	1.595	1.276	NF5	1.500	2.681	2.045	3.560
FF6	1.500	2.134	1.845	1.891	NF6	1.500	2.497	1.885	2.822
FF7	1.500	1.768	1.767	1.325	NF7	1.500	2.689	1.974	3.594
average	1.500	1.682	1.802	1.299	average	1.500	2.430	1.984	2.716

Regarding the comparison between the virgin and scragged cases, in order to explain the different trends observed in the results it may be useful to note first that the FF records are characterized by displacement response spectra which remain constant (Fig. 18e) or increase (Fig. 18f) for increasing period, whereas NF records are always characterized by displacement spectra which increase significantly at large periods (Fig. 19e and Fig. 19f). In the case of FF records with constant spectra, although the scragged and virgin devices have different dynamic properties and relevant effective vibration periods, they undergo similar displacements. Thus, the scragged device being more flexible, the maximum stresses attained in the scragged case are smaller (see FF1, FF2, FF3 in Table 4 and Fig. 18a). In contrast, in the case of FF records with increasing displacement spectra at large periods, the scragged bearing system, characterized by a higher effective period, undergoes larger displacements than the virgin one. However, in the cases where the softening is maximum (i.e., several cycles taking place before the largest one) the differences in terms of strain demand between the virgin and scragged case are not very large and the maximum stresses attained by the scragged device remain smaller (Fig. 18b and FF5, FF7 in Table 4). Conversely, in the cases in which the softening is limited (i.e. few small-amplitude cycles taking place before the largest one)

the differences in terms of strain demand between the virgin and scragged cases are high (see FF4, FF6 in Table 4) and the maximum stresses achieved by the scragged device are significantly larger. Moreover, it is noted that despite the differences in the numbers of cycles for the various records, the damage parameters never attain the limit value for the design strain (Fig. 18c,d).

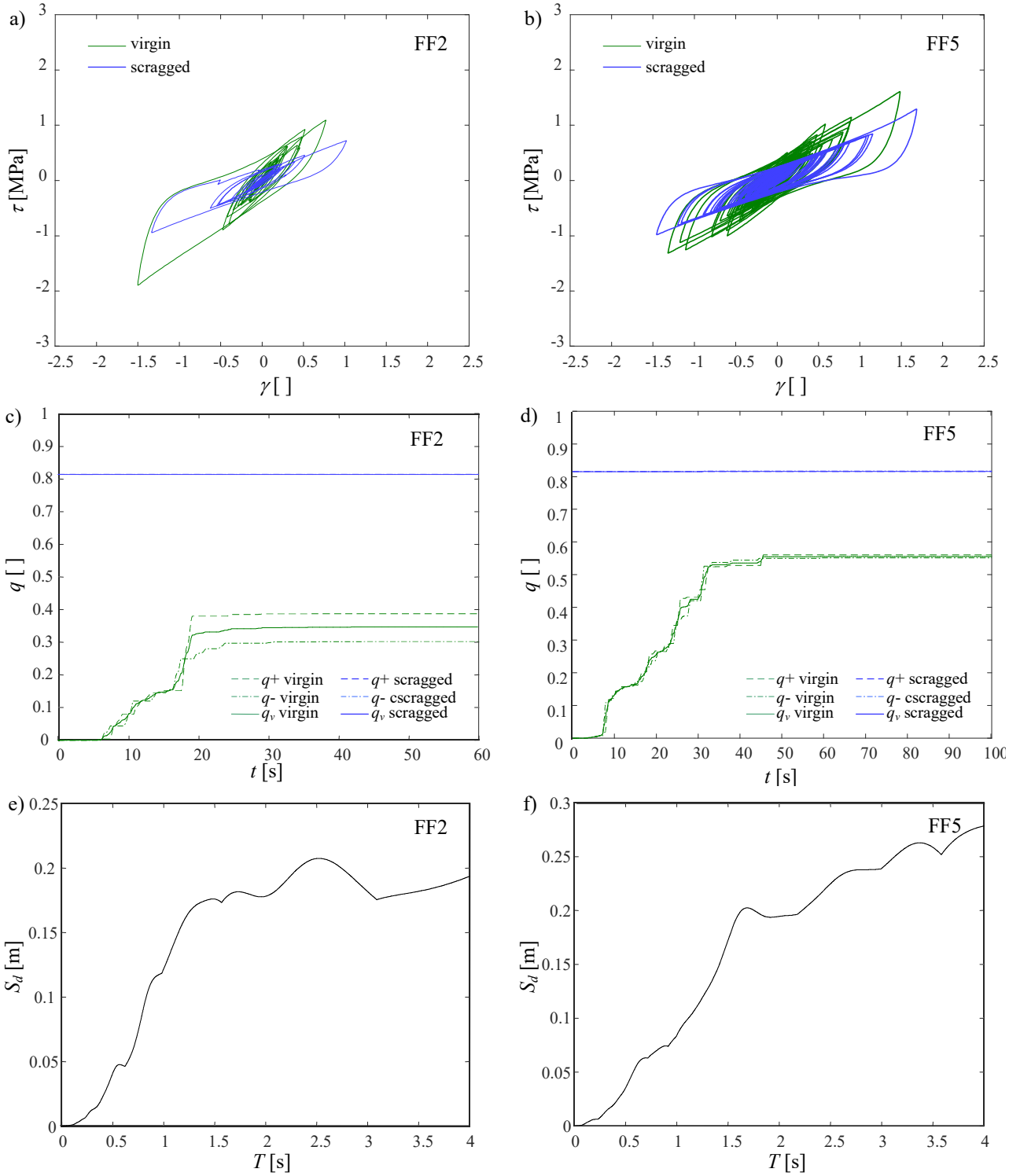

Fig. 18 – Result of the analyses for two FF records: shear stress-strain response of virgin and scragged isolators (a,b), evolution of damage parameters (c,d), 5% damped elastic displacement response spectra (e,f).

Under the action of NF ground motions, as a consequence of the combined effects of load paths with minimal softening (see Fig. 19c,d), and of displacement spectra that increase significantly with the period, the response in terms of maximum strain of the scragged bearing is always significantly larger than the response of the virgin device, as is observed in Fig. 19a (representative of the response to NF2, NF3, NF4 records in Table 4), or even more clearly in Fig.19b (representative of

the response to NF1, NF5, NF6 and NF7 records in Table 4), where a strain amplitude in the range of the stiffening response of the rubber is attained by the scragged bearing. In the first case, the maximum shear stresses of the virgin and scragged devices are similar to each other, whereas in the second case the shear stress experienced by the scragged bearing is significantly larger. Note that in both the cases, the maximum strain significantly exceeds the design strain equal to 1.5, thus also the damage parameters in the scragged response attains values beyond the limit value 0.82 (Fig. 19c,d).

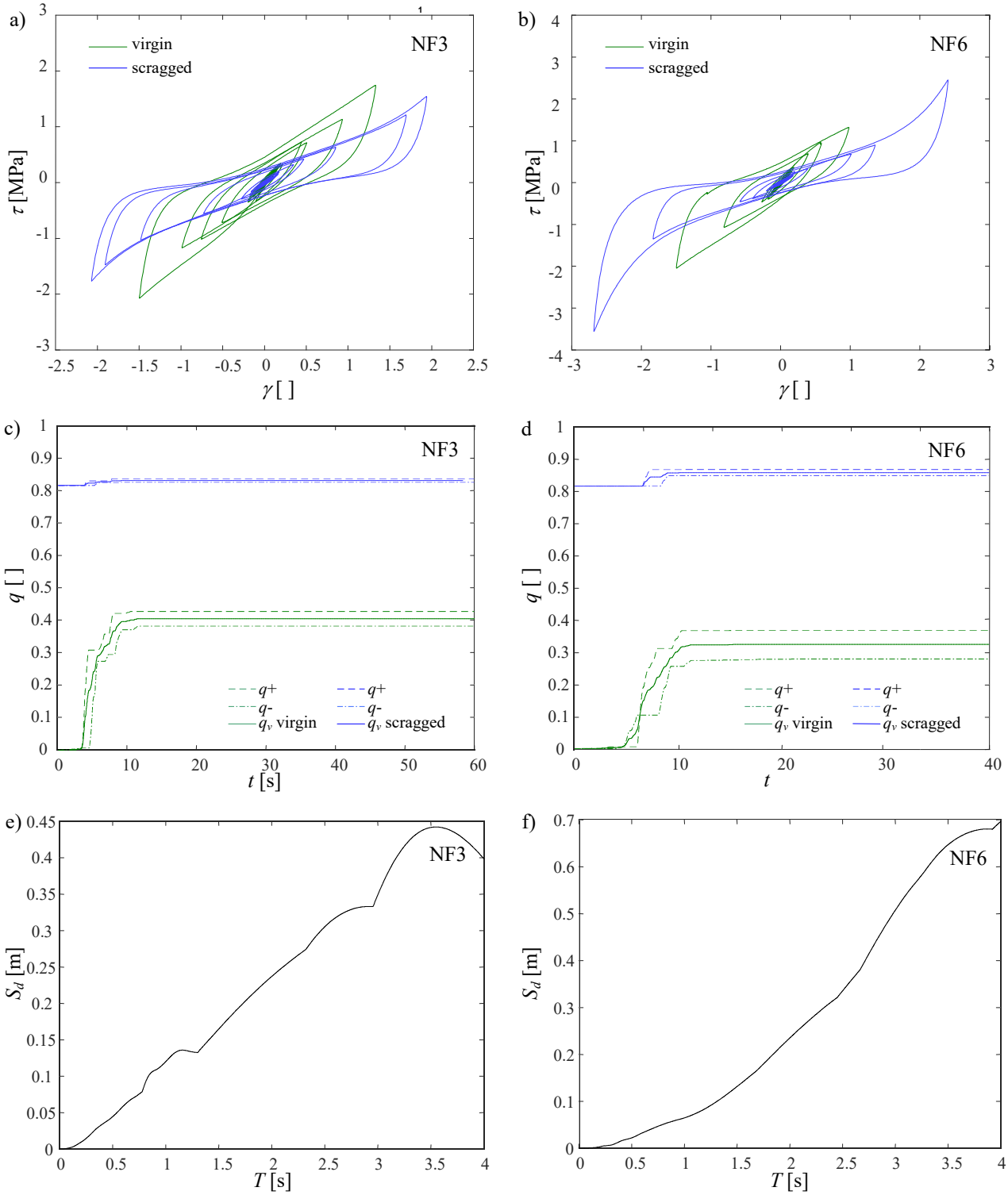

Fig. 19 – Result of the analyses for two NF records: shear stress-strain response of virgin and scragged isolators (a,b), evolution of damage parameters (c,d), 5% damped elastic displacement response spectra (e,f).

On average, in the case of FF motions the maximum strain is 12% lower for the virgin case than for the scragged case, whereas the maximum stress is 27% larger. Thus, as expected, modelling the rubber in its scragged state leads to an overestimation of the displacements and an underestimation of the stress of the bearing and thus of the forces transmitted to the isolated superstructure. However, the difference between the forces is limited (lower with respect to the ratio between the maximum stresses of the first and tenth cycle at the design strain amplitude, which is about 1.6) because of the smaller displacements attained by the model for virgin rubber behaviour. In contrast, in the case of NF records, both the average strain and the average stress are smaller in the case where virgin rubber properties are considered. In particular, the normalized differences are respectively 62% for the strain and 37% for the stress. This result is of particular interest because NF earthquakes are very critical for isolated systems in consequence of the large displacements that they can induce [41-42] but accounting for stress softening from the virgin state during simulated responses predicts significant reduction of this negative effect. It is worth noting that NF ground motions are still critical also by considering the Mullins effect, since the scale factors reported in Table 3 are all lower than 1 in order to maintain the design displacement at 0.2 m. Instead, if the bearings had to be designed to the unscaled ground motions, a larger design displacement or an additional damping source would be required, but the same differences would be observed between the cases with and without the stress softening. Furthermore, it is worth mentioning that results presented in this section are only qualitative and focused on the influence of the shear stress softening on the seismic response of isolated structures. A more complete and accurate analysis would consider: (i) multiple degrees of freedom model of the structural system, (ii) the actual multi-axial behaviour of HDNR isolators calibrated on the basis of experimental tests on bearing prototypes, (iii) all checks prescribed by current seismic codes for the building and the isolation devices.

CONCLUSIONS

This paper addresses experimental and numerical investigations carried out to better understand and model the stress-softening behaviour of high-damping natural rubber (HDNR) and its impact on the seismic response of isolated systems.

The experimental campaign, carried out at TARRC on a wide set of virgin HDNR pieces, has been tailored to study some aspects related to the stress-softening effect which have received minor attention in the past, such as the direction-dependence and the recovery properties, and to characterize the transient (i.e. softening) and stable (i.e. fully scragged) behaviour of a HDNR compound commonly used for isolation bearings under different strain histories. The test results have been used to devise and fit a model for simulating the rubber behavior in shear, which advances the state of the art in the description of the transient behavior and which can be used to describe the horizontal shear behavior of virgin HDNR bearings for typical values of shape factors and design actions. Near the collapse conditions the bearing behavior is more complex, however the proposed model can be used to improve the description of the horizontal virgin behavior in more complex coupled multiaxial models of bearings. In particular, with reference to the transient response, two damage parameters have been introduced to describe the uniaxial but direction-dependent (i.e. positive or negative) damage process affecting the elastic response contribution, and a further damage parameter to describe the damage process affecting the dissipative contribution. The proposed model has been used to analyse the seismic response under the design condition of a simplified isolated structure modelled as a S-DOF system subjected to ground motions with different characteristics for the isolators: either the virgin condition, with consequent softening during the excitation, and the scragged condition, without such transient softening. The results show that, except for the special case of NF ground motions, the scragged condition, considered less realistic albeit easier to model, leads to an overestimation of the bearing displacements and an underestimation of the forces acting on the bearings and thus transmitted to the structure. However,

the obtained differences are not large, suggesting simplified approaches, taken by Eurocode 8 and other international seismic codes such as AASHTO 2010 or ASCE/SEI 41-139 based on safety factors or property modification factors applied to simple elasto-plastic or visco-elastic models could be justified, thus accounting indirectly for the consequences of the Mullins effect and its possible recovery. In contrast, in the case of NF records, usually considered very critical for isolated systems, the results show that simulations based on the scragged condition result in very large displacements, often attaining the range of the stiffening response of the rubber, and to very high bearing stresses. Nevertheless, NF ground motions remain a challenge for the design of isolated structures even with stress softening taken into account, as a large design displacement or additional damping source is likely to be called for. In any case, the use of models accounting for the virgin condition and consequent stress-softening during the seismic excitation due to NF records is recommended to have a reliable estimate of the bearing displacements and of the eventual additional damping required. Furthermore, further studies should be carried out by employing more accurate building models as well as the actual distribution and multi-axial behaviour of bearings.

AKNOWLEDGEMENTS

The study reported in this paper was sponsored by the Tun Abdul Razak Research Centre (TARRC) and by the Italian Department of Civil Protection within the Reluis-DPC Projects 2016. The authors gratefully acknowledge this financial support.

REFERENCES

1. Mullins L. Softening of rubber by deformation, *Rubber Chemistry and Technology* 1969, **42**(1): 339-362.
2. Govindjee S, Simo J. Mullins effect and the strain amplitude dependence of the storage modulus. *International Journal of Solids and Structures* 1992, **29**(14-15):1737-1751.
3. Kingston J.G.R., Muhr A.H. Effect of scragging on parameters in viscoplastic model for filled rubber. *Plastics, Rubber and Composites* 2011, **40**(4): 161-168.
4. Muhr A.H., Modelling the stress-strain behavior of rubber, *Rubber Chemistry and Technology* 2005, 78(3): 391-42.
5. Miehe C., Keck J. Superimposed finite elastic–viscoelastic–plastoelastic stress response with damage in filled rubbery polymers. Experiments, modelling and algorithmic implementation. *Journal of the Mechanics and Physics of Solids* 2000; **48**(2): 323-365.
6. Clark PW, Aiken ID, Kelly JM. *Experimental studies of the ultimate behaviour of seismically isolated structures*, Report No. UCB/EERC-97/18, Earthquake Engineering Research Center, University of California, Berkeley, California, 1997.
7. Kulak RF, Coveney VA, Jamil S. *Recovery characteristics of high-damping elastomers used in seismic isolation bearings, Seismic, Shock, and Vibration Isolation*, ASME Publication PVP-Vol. 379, American Society of Mechanical Engineers, Washington, D.C. 1998.
8. Constantinou MC, Tsopelas, P, Kasalanati A, Wolff E. *Property modification factors for seismic isolation bearings*, Technical Report MCEER-99-0012, Multidisciplinary Center for Earthquake Engineering Research, Buffalo, New York, 1999.
9. Thomson AC, Whittaker AS, Fenves GL, Mahin SA. Property modification factors for elastomeric seismic isolation bearings. *Proceedings of the 12th World Conference on Earthquake Engineering*, New Zealand, Auckand, 2000.
10. Stewart JP, Conte JP, Aiken ID. Observed behaviour of Seismically Isolated Buildings, *Journal of Structural Engineering* 1999, **125**(9):955-964.
11. Oliveto ND, Scalia G, Oliveto G. Time domain identification of hybrid base isolation systems using free vibration tests. *Earthquake Engineering & Structural Dynamics* 2010; **39**(9): 1015-1038.
12. Govindjee S, Simo J. A micro-mechanically based continuum damage model for carbon black-filled rubbers incorporating Mullins' effect. *Journal of the Mechanics and Physics of Solids* 1991, **39**(1): 87–112.
13. Lion A. A constitutive model for carbon black filled rubber: Experimental investigation and mathematical representation. *Continuum Mechanics and Thermodynamics* 1996, **8**(3):153–169.
14. Haupt P, Sedlan K. Viscoplasticity of elastomeric materials: experimental facts and constitutive modeling. *Archive of Applied Mechanics* 2001, **71**(2-3):89-109.
15. Dorfman A, Ogden RW. A constitutive model for the Mullins effect with permanent set in particle-reinforced rubber, *International Journal of Solids and Structures* 2004, **41**:1855–1878
16. Montuori G.M., Mele E., Marrazzo G., Brandonisio G., De Luca A. Stability issues and pressure–shear interaction in elastomeric bearings: the primary role of the secondary shape factor, Bulletin of Earthquake Engineering 2016, **14**:569–597.

17. Kelly J.M., Konstantinidis D. Mechanics of Rubber Bearings for Seismic and Vibration Isolation. John Wiley & Sons, Ltd. 2011.
18. Ahmadi HR, Fuller KNG, Muhr AH. Predicting response of non-linear high damping rubber isolation systems, *Proceedings of the Eleventh World Conference on Earthquake Engineering*, Acapulco, Mexico. 1996.
19. Kikuchi M, Aiken ID. An Analytical Hysteresis Model for Elastomeric Seismic Isolation Bearings, *Earthquake Engineering and Structural Dynamics* 1997, **26**(2):215-231.
20. Hwang JS, Wu JD, Pan .C, Yang G. A Mathematical Hysteretic Model for Elastomeric Isolation Bearings. *Earthquake Engineering and Structural Dynamics* 2002, **31**(4): 771-789.
21. Tsai CS, Chiang TC, Chen BJ, Lin SB. An Advanced Analytical Model for High Damping Rubber Bearings, *Earthquake Engineering and Structural Dynamics* 2003, **32**(9):1373-1387.
22. Dall'Asta A, Ragni L. Experimental Tests and Analytical Model of High Damping Rubber Dissipating Devices, *Engineering Structures* 2006, **28**(13):1874-1884.
23. Abe M, Yoshida J, Fujino Y. Multiaxial Behaviours of Laminated Rubber Bearings and their Modeling. II: Modelling, *Journal of Structural Engineering* 2004, **130**(8):1133-1144.
24. Grant DN, Fenves GL, Whittaker AS. Bidirectional modeling of high-damping rubber bearings. *Journal of Earthquake Engineering* 2004, **8**(1):161-185.
25. Grant DN, Fenves GL, Auricchio F. Modelling and analysis of High-damping Rubber Bearings for the seismic protection of bridges. Iuss Press, Pavia, 2005.
26. Yamamoto S, Kikuchi M, Ueda1 M, Aiken IA. A mechanical model for elastomeric seismic isolation bearings including the influence of axial load. *Earthquake Engineering And Structural Dynamics* 2009, **38**:157–180
27. Kikuchi M, Nakamura T, Aiken ID. Three-dimensional analysis for square seismic isolation bearings under large shear deformations and high axial loads. *Earthquake Engineering and Structural Dynamics* 2010, **39**:1513–1531
28. Kumar M. *Seismic isolation of nuclear power plants using elastomeric bearings*. PhD Dissertation, Departement of Civil, Structural and Environmental Engineering, University at Buffalo, 2015.
29. Diercks N, Lion A. Modeling deformation-induced anisotropy using 1D-laws for Mullins-Effect. *Constitutive models for rubber VIII*, Taylor & Francis Group, London 2013, pp.419-424.
30. Wulf H, Ihlemann J. Simulation of self-organization processes in filled rubber and their influence on anisotropic Mullins effect. *Constitutive models for rubber VIII*, Taylor & Francis Group, London 2013, pp.425-430.
31. Dall'Asta A, Ragni L. Nonlinear behavior of dynamic systems with high damping rubber devices, *Engineering Structures* 2008a, **30**(12):3610-3618.
32. Dall'Asta A, Ragni L. Dynamic systems with high damping rubber: Nonlinear behaviour and linear approximation, *Earthquake Engineering and Structural Dynamics* 2008b, **37**(13):1511-2526.
33. European Committee for Standardization (ECS). *EN 15129:2009, Anti-seismic devices*, CEN, Bruxelles, 2009.
34. American Association of State Highway and Transportation Officials (AASHTO). Guide specifications for seismic isolation design, Washington, D.C., 2010
35. American Society of Civil Engineers (ASCE). A*SCE/SEI 41-13: Seismic Rehabilitation of Existing Buildings*. Reston, Virginia, 2014.
36. International Organization for Standardization (ISO). ISO 4664-1:2011 Rubber, vulcanized or thermoplastic - Determination of dynamic properties - Part 1: General guidance, Geneva, 2011.
37. Ozdemir H. *Nonlinear transient dynamic analysis of yielding structures*. PhD dissertation, University of California, Berkeley, 1973.
38. Huang W-H. Bi-Directional Testing, Modeling, and System Response of Seismically Isolated Bridges. Ph. D. thesis, University of California, Berkeley, 2002.
39. Dafalias Y, Popov E. A model for nonlinearly hardening materials for complex loading. *Acta Mechanica* 1975, 21 (3): 173-192.
40. Osterlof R., Wentzel H., Kari L., Diercks N., Wollscheid D. Constitutive modeling of the amplitude and frequency dependency of filled elastomers utilizing a modified Boundary Surface Model. *International Journal of Solids and Structures* 2014, **51**: 3431–3438
41. Jangid R. S., Kelly J. M. Base isolation for near-fault motions. *Earthquake Engineering and Structural Dynamics* 2001, **30**:691-707.
42. Mazza F., Vulcano A. Nonlinear Response of RC Framed Buildings with Isolation and Supplemental Damping at the Base Subjected to Near-Fault Earthquakes. *Journal of Earthquake Engineering* 2009, **13**(5):690-715.